Neurobiology of Aging 111 (2022) 24–34

Contents lists available at ScienceDirect

Neurobiology of Aging

journal homepage: www.elsevier.com/locate/neuaging.org

Brain network modulation in Alzheimer's and frontotemporal dementia with transcranial electrical stimulation

Lorenzo Pini[a,b], Francesca Benedetta Pizzini[c,†], Ilaria Boscolo-Galazzo[d,†], Clarissa Ferrari[e], Samantha Galluzzi[a], Maria Cotelli[f], Elena Gobbi[f], Annamaria Cattaneo[g,h], Maria Sofia Cotelli[i], Cristina Geroldi[j], Orazio Zanetti[j], Maurizio Corbetta[b,k], Martijn van den Heuvel[l], Giovanni Battista Frisoni[a,m], Rosa Manenti[f], Michela Pievani[a,*]

[a] Laboratory Alzheimer's Neuroimaging & Epidemiology, IRCCS Istituto Centro San Giovanni di Dio Fatebenefratelli, Brescia, Italy
[b] Department of Neuroscience & Padova Neuroscience Center, University of Padova, Padova, Italy
[c] Radiology, Department of Diagnostic and Public Health, University of Verona & Department of Diagnostics and Pathology, University Hospital, Verona, Italy
[d] Department of Computer Science, University of Verona, Verona, Italy
[e] Unit of Statistics, IRCCS Istituto Centro San Giovanni di Dio Fatebenefratelli, Brescia, Italy
[f] Neuropsychology Unit, IRCCS Istituto Centro San Giovanni di Dio Fatebenefratelli, Brescia, Italy
[g] Biological Psychiatric Unit, IRCCS Istituto Centro San Giovanni di Dio Fatebenefratelli, Brescia, Italy
[h] Department of Pharmacological and Biomolecular Sciences, University of Milan, Milan, Italy
[i] Neurology Unit, Valle Camonica Hospital, Brescia, Italy
[j] Alzheimer's Unit - Memory Clinic, IRCCS Istituto Centro San Giovanni di Dio Fatebenefratelli, Brescia, Italy
[k] Venetian Institute of Molecular Medicine, VIMM, Padova, Italy
[l] Center for Neurogenomics and Cognitive Research, Vrije Universiteit Amsterdam, Amsterdam, Netherlands
[m] Memory Clinic and LANVIE-Laboratory of Neuroimaging of Aging, University Hospitals and University of Geneva, Geneva, Switzerland

ARTICLE INFO

Article history:
Received 24 June 2021
Revised 15 November 2021
Accepted 16 November 2021
Available online 20 November 2021

Keywords:
Alzheimer's disease
Frontotemporal dementia
Network stimulation
Default mode network
Salience network

ABSTRACT

The default mode (DMN) and the salience (SN) networks show functional hypo-connectivity in Alzheimer's disease (AD) and the behavioral variant of frontotemporal dementia (bvFTD), respectively, along with patterns of hyper-connectivity. We tested the clinical and neurobiological effects of noninvasive stimulation over these networks in 45 patients (AD and bvFTD) who received either anodal (target network: DMN in AD, SN in bvFTD) or cathodal stimulation (target network: SN in AD, DMN in bvFTD). We evaluated changes in clinical, cognitive, functional and structural connectivity, and perfusion measures. In both patient groups, cathodal stimulation was followed by behavioral improvement, whereas anodal stimulation led to cognitive improvement. Neither functional connectivity nor perfusion showed significant effects. A significant interaction between DMN and SN functional connectivity changes and stimulation protocol was reported in AD. These results suggest a protocol-dependent response, whereby the protocols studied show divergent effects on cognitive and clinical measures, along with a divergent modulatory pattern of connectivity in AD.

© 2021 The Authors. Published by Elsevier Inc.
This is an open access article under the CC BY-NC-ND license
(http://creativecommons.org/licenses/by-nc-nd/4.0/)

1. Introduction

Alzheimer's disease (AD) and the behavioral variant of frontotemporal dementia (bvFTD) are 2 major causes of neurodegeneration, involving a progressive decline in cognitive abilities and behavioral control, ultimately leading to loss of functional capacity (Ferri et al., 2005; Neary et al., 2005). These diseases involve multiple complex mechanisms, from abnormal protein deposition (i.e., amyloid and hyperphosphorylated tau in AD; tau, TAR DNA binding protein-43 or fused-in-sarcoma (FUS) pathology in FTD) to

Abbreviations: AD, Alzheimer's disease; ASL, arterial spin labeling; bvFTD, behavioral variant frontotemporal dementia; DMN, default mode network; FC, functional connectivity; rs-fMRI, resting-state functional magnetic resonance imaging; SN, salience network.

* Corresponding author at: M. Pievani, Laboratory Alzheimer's Neuroimaging & Epidemiology, IRCCS Istituto Centro San Giovanni di Dio Fatebenefratelli, Via Pilastroni 4, Brescia 25125, Italy. Tel. +39 030 3501361, Fax +39 030 3501592
E-mail address: mpievani@fatebenefratelli.eu (M. Pievani).
† These authors contributed equally to this work.

0197-4580/$ – see front matter © 2021 The Authors. Published by Elsevier Inc. This is an open access article under the CC BY-NC-ND license (http://creativecommons.org/licenses/by-nc-nd/4.0/)
https://doi.org/10.1016/j.neurobiolaging.2021.11.005

neuronal dysfunction, inflammation, and neuronal loss (DeTure and Dickson, 2019; Mackenzie and Neumann, 2016). While a large body of research has focused on the molecular hallmarks of diseases, less attention has been paid to the mechanisms of network dysfunction, which might represent an alternative therapeutic target (Palop and Mucke, 2016). It has been hypothesized that toxic proteins may spread across functional networks through a "prion-like" mechanism in neurodegenerative diseases (Buckner et al., 2005; Pini et al., 2020; Seeley et al., 2009; Zhou et al., 2010). Functional networks can be quantified noninvasively with resting-state functional magnetic resonance imaging (rs-fMRI). This technique measures the relationship between the blood oxygenation level dependent (BOLD) signal between different regions. Brain areas showing temporal correlation in BOLD levels are functionally related and are commonly referred to as "networks" (Biswal et al., 1995). These circuits might provide the functional scaffolding of cognitive and social abilities (Laird et al., 2011; Pezzulo et al., 2021; Shine et al., 2016). Different cortical networks support specific abilities, such as the default mode network (DMN) for memory (Ranganath and Ritchey, 2012) or the salience network (SN) for attention, social cognition, emotion control and behavior regulation (Menon and Uddin, 2010). Similarly, their functional breakdown is linked to cognitive impairment in several neurological disorders, including AD and bvFTD (Seeley et al., 2009; Buckner et al., 2005; Zhou et al., 2010; Pini et al., 2021). Aberrant functional connectivity (FC) of the DMN is a well-established feature in AD and is associated with clinical severity and episodic memory impairment (Buckner et al., 2005; Zhang et al., 2010). In bvFTD, reduced FC within the SN is associated with clinical symptoms (Seeley et al., 2009; Day et al., 2013). Moreover, brain regions belonging to DMN and SN exhibit distinct alterations in the cerebral blood flow (CBF) in AD and bvFTD (Benedictus et al., 2017; Hu et al., 2010).

Abnormal network connectivity is emerging as a promising target for intervention in neurodegenerative diseases. We and others have previously proposed that functional neuroimaging could help guide the implementation of brain stimulation paradigms (Fox et al., 2014; Pievani et al., 2016; Sale et al., 2015). Noninvasive brain stimulation (NIBS) is the method of choice to directly alter brain activity by increasing or reducing cortical excitability (Sandrini et al., 2011). The 2 most common NIBS interventions are repetitive transcranial magnetic stimulation (rTMS) and transcranial direct current stimulation (tDCS). rTMS can perturb network dynamics by increasing or decreasing cortical excitability, whereas during tDCS a weak electrical current is applied directly to specific regions to modulate neuronal membrane potentials with excitatory or inhibitory effects depending on polarity (Bikson et al., 2013; Sandrini et al., 2011). These techniques could be used to modulate FC of cortical networks, with both local and distal effects in brain circuits (Fox et al., 2014). To date, several studies have combined NIBS with rs-fMRI in healthy individuals showing that the propagation of NIBS-induced perturbation follows pathways that are functionally or structurally connected with the stimulation target (Ozdemir et al., 2020; Schintu et al., 2020). Consistent modulation of FC has been reported after NIBS, with both local and distal effects (Amadi et al., 2014; Ozdemir et al., 2020; Lindenberg et al., 2016; Stagg et al., 2014). These effects could be mediated by modulation of GABAergic and glutamatergic pathways, although further studies are needed to shed light on the microscale effects of both rTMS and tDCS (see (Pini et al., 2018) for a comprehensive review).

To date, several studies have investigated NIBS-induced clinical and cognitive changes in neurodegenerative disorders, without focusing specifically on brain networks, and their efficacy has not yet been demonstrated (Lefaucheur et al., 2017; 2020). Only a few studies have assessed NIBS-induced modulation of connectivity in AD or FTD. Meinzer et al. (2015) reported in patients with mild cognitive impairment a "normalization" of FC after anodal tDCS in brain regions involved in the language network (i.e., the left inferior frontal gyrus). Recently, Koch and colleagues (2018) adopted the electroencephalography (EEG)-TMS approach to investigate the effect of high-frequency rTMS of the precuneus, a key node of the DMN, in prodromal AD patients, reporting improved memory and changes in EEG-based DMN connectivity (Koch et al., 2018). In line with these studies suggesting that NIBS can modulate network connectivity, our aim was to investigate whether NIBS can (1) enhance connectivity and perfusion of the networks affected in AD and bvFTD (i.e., DMN and SN, respectively), (2) improve clinical and cognitive measures. Compared with previous EEG-TMS studies, we will employ multimodal MRI to assess functional and structural connectivity with rs-fMRI and diffusion MRI, and perfusion with arterial spin labeling (ASL).

Furthermore, DMN and SN show divergent patterns in the healthy brain (i.e., when the SN is activated, the DMN is deactivated, and vice versa; Sridharan et al., 2008). Similarly, anticorrelated connectivity patterns are observed in AD and bvFTD, with reduced DMN connectivity in AD accompanied by hyper-synchrony in the SN, and, conversely, reduced SN connectivity in bvFTD by DMN hyper-synchrony (Zhou et al., 2010). Based on these relationships, we hypothesize that NIBS interventions aimed at inhibiting anticorrelated networks might induce similar effects to approaches aimed at enhancing hypo-connected networks.

The aim of the study was, therefore, to test the effect of tDCS on clinical, cognitive, structural and functional connectivity, and perfusion features in AD and bvFTD by implementing 2 paradigms, 1 aimed at excitation of the hypo-connected network (i.e., the DMN in AD, and the SN in bvFTD), and 1 at inhibition of the anticorrelated network (i.e., the SN in AD, and the DMN in bvFTD).

2. Methods

2.1. Participants and study design

This study was conducted in accordance with the principles of the Declaration of Helsinki. Patients were enrolled at the IRCCS Istituto Centro San Giovanni di Dio Fatebenefratelli in Brescia (Italy) and underwent clinical, cognitive, and imaging assessment at baseline (T0) and after 3 weeks (T1). See Fig. 1 for a flowchart of the study. Patients were also evaluated after 6 months (T2 follow-up); these data were not included in the current investigation. Biological samples (blood) were collected for APOE genotyping. Clinical, cognitive, and imaging variables were collected only once (T0) in age-matched healthy controls (HC) recruited through advertising or among caregivers.

Inclusion criteria were a clinical diagnosis of AD or bvFTD (McKhann et al., 2011; Rascovsky et al., 2011), age between 50 and 85 years, ability to provide written informed consent, and availability of a collateral source. Exclusion criteria for patients were (1) moderate/severe dementia (Mini Mental State Examination - MMSE score <18), (2) any medical condition that could interfere with evaluations, (3) contraindications for MRI and tDCS (metal implants, pacemakers, prosthetic heart valves, claustrophobia, epilepsy). Additionally, patients with cortical vascular lesions on MRI were excluded for tDCS safety. The concomitant use of drugs was not an exclusion criterion, but patients had to be on a stable dosage regimen for at least 12 weeks before inclusion and until the end of the study. Eventual changes in therapy were monitored during the study. Exclusion criteria for HC were a medical history of neurologic or psychiatric conditions that could interfere with the assessment (e.g., transient ischemic attack, stroke, head trauma, epilepsy, multiple sclerosis, neuropathy, mood disorders, substance abuse) plus contraindications for MRI.

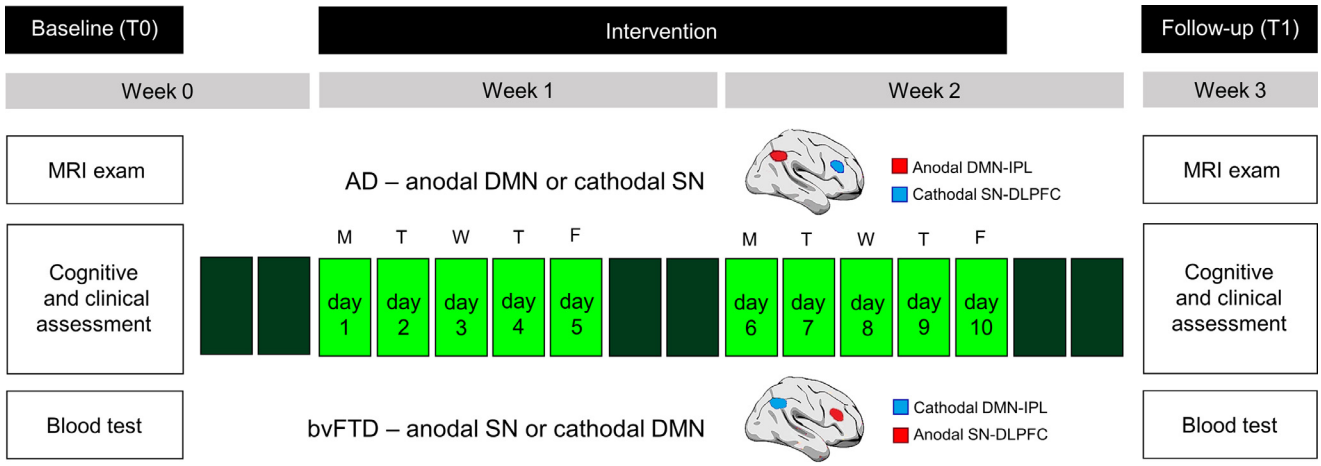

Fig. 1. Experimental design of the study. Patients underwent an extensive clinical/cognitive assessment and a multimodal MRI exam at week 0 (baseline). This baseline evaluation was followed by 2 weeks of intervention. At week 3, patients underwent the same cognitive/clinical and MRI exam as follow-up.

2.2. Study procedures

2.2.1. Randomization and sample size calculation

Upon inclusion, participants were randomly assigned to 2 groups (1:1 ratio): (1) anodal tDCS stimulation of the DMN in AD (aDMN protocol) and of the SN in bvFTD (aSN protocol), or (2) cathodal tDCS stimulation of the SN in AD (cSN protocol) and of the DMN in bvFTD (cDMN protocol). A covariate adaptive randomization procedure was adopted to control for disease severity and age by dichotomizing both variables into 2 categories (MMSE cutoff: 21 for AD, 24 for bvFTD; age cutoff: 70 years) (Lin et al., 2016).

The sample size for this pilot study (n = 10 per group) was estimated based on a previous study assessing FC changes in the DMN in AD patients after pharmacological intervention (Lorenzi et al., 2011). Moreover, based on a study using multi-session application of excitatory rTMS to modulate FC of DMN hubs in adults (Wang et al., 2014), we estimated that this sample size would provide at least 90% power to detect a 0.9 ± 0.85 difference (effect size of 1.06) in FC of the DMN after rTMS at the significance level of 0.05 using a 2-sided paired t-test. These studies were selected based on their commonalities with our study, such as the same outcome measure (DMN connectivity; Lorenzi et al., 2011) or the similar intervention (multi-session modulation of the DMN through a NIBS approach; Wang et al., 2014). Moreover, this sample size is largely overlapping with several previous studies investigating tDCS-induced effects in patients with dementia (see Table 3 in (Pini et al., 2018).

Patients, caregivers, and all study staff involved in the assessment were blinded to group assignment at the conclusion of follow-up. Patients were aware of the position of the electrodes on the skull, but not of the polarity of stimulation. Caregivers were blinded to the entire procedure. The researchers responsible for tDCS were blind to the clinical and cognitive characteristics of the patients.

2.2.2. tDCS procedures

Each patient underwent 10 daily 25-minutes tDCS sessions (fade-in and fade-out periods = 10 seconds) over 2 weeks. tDCS was delivered by a battery-powered constant current stimulator (BrainStim, EMS, Bologna, Italy) connected to a pair of sponge electrodes (anode and cathode). The size of the anode/cathode was based on whether the electrode was the 'target' (5 × 5 cm^2) or the "reference" (6 × 8 cm^2). The reference electrode was larger than the target electrode to improve the focality of the stimulation. The current intensity was set to 1.5 mA, leading to a maximum of 0.06 mA/cm2 current intensity under the target electrode, within safety limits (Poreisz et al., 2007). The electrodes were secured using elastic bands, and to reduce contact impedance an electro-conductive gel was applied under the electrodes. No cognitive tasks were administered. Patients were asked to remain seated and relaxed during the whole stimulation session.

The target electrode was positioned according to the results of a previous meta-analysis of DMN and SN rs-fMRI studies (Pievani et al., 2017). For the aDMN protocol, the target (anode) was placed over the right inferior parietal DMN node (P4-P6 on the EEG 10/20 system), whereas the reference (cathode) was placed over the contralateral supraorbital region. For the cSN protocol, the target (cathode) was positioned over the right dorsolateral prefrontal SN node (Fp2-AF4), whereas the reference (anode) was positioned over the inion. In bvFTD, the same configuration was used, but the polarity of the electrodes was reversed: for the aSN protocol, the anode was placed over the right dorsolateral prefrontal SN hub (Fp2-AF4) and the cathode over the inion; for the cDMN protocol, the cathode was placed over the right inferior parietal DMN lobe (P4-P6) and the anode over the contralateral supraorbital cortex. Supplementary Figure S1 shows the tDCS montage for the 4 tDCS protocols, and Supplementary Figure S2 shows the tDCS current flow modeling.

2.3. Cognitive and clinical assessment

The neuropsychological evaluation assessed: global cognition with the MMSE (Folstein et al., 1975); memory with Auditory Verbal Learning Test, immediate and delayed recall (Carlesimo et al., 1996), Rey–Osterrieth Complex Figure recall (Caffara et al., 2002), story recall (Novelli et al., 1986a), digit span backward and forward tests (Monaco et al., 2013) and the paired associates learning test; language with verbal fluency (phonemic and semantic) tasks (Novelli et al., 1986b), and Token Test (Spinnler and Tognoni 1987); attention and executive functions with Trail Making Test part A and part B (Amodio et al., 2002; Giovagnoli et al., 1996) visuo-constructional abilities with Rey–Osterrieth Complex Figure copy (Caffara et al., 2002) and the clock test (Caffara et al., 2011); emotion recognition with the Reading the Mind in the Eyes (Serafin and Surian, 2004), and the 60 Ekman faces tests (Dodich et al., 2014). Controls underwent cognitive evaluation only at baseline, for comparison purposes, whereas patients repeated the cognitive evaluation at all time points considered. Finally, we

computed composite scores for each cognitive domain (i.e., memory, language, executive, visuo-constructional and emotion recognition). To this aim, patients' scores on each test were z-transformed according to the performance distribution of the HC sample. Z-scores from each test were then averaged for each domain.

The clinical battery included the Clinical Dementia Rating (CDR) Scale (global and sum of boxes (CDR-SOB) scores) (Hughes et al., 1982), the Neuropsychiatric Inventory (NPI) (Cummings et al., 1994), and the Frontal Behavior Inventory (FBI, for bvFTD only) (Kertesz et al., 1997). In addition, the following clinical scales were collected to evaluate disease severity: Barthel index (Mahoney and Barthel, 1965), Instrumental Activities of Daily Living scale (IADL) (Lawton and Brody 1969), Geriatric Depression Scale (GDS) (Yesavage et al., 1982).

2.4. MRI acquisition protocol

Rs-fMRI, diffusion MRI, and ASL data were acquired on a 3T Philips Achieva system equipped with an 8-channel head-coil (University Hospital of Verona, Italy). The following sequences and parameters were used: 2D gradient echo echo-planar imaging (GRE-EPI) sequence for functional connectivity analysis (time repetition (TR)/echo time (TE) = 3000/30ms; flip angle = 80°, resolution = 3mm isotropic; 48 axial slices; volumes = 200); 2D GRE-EPI pseudo-continuous ASL for CBF measurement (TR/TE = 4376/12 ms; labeling duration/postlabeling delay = 1650/1800ms, 2 background suppression pulses at 1700 ms and 2926 ms from the start of the scan; flip angle = 90°; resolution = 3 × 3 × 4 mm^3; 26 slices; volumes = 90); 3D structural T1-weighted (TR/TE = 8/3.7 ms; flip angle = 8°; resolution = 1 mm isotropic; 180 sagittal slices); 2D fluid attenuated inversion recovery for white matter hyperintensities (WMHs) assessment (TR/TE = 9000/90 ms; TI = 2500 ms; flip angle = 150°; resolution = 0.86 × 0.86 × 5 mm3; 35 axial slices). Finally, diffusion data were acquired using an axial spin-echo EPI sequence (TR/TE = 10269/55 ms; flip angle = 90°; resolution = 2mm isotropic; 60 axial slices; b-value = 1000 s/mm^2; 32 directions plus 1 b = 0 s/mm^2). Additionally, a calibration scan with the same parameters as the ASL sequence but with a longer TR (10s) and without background suppression was acquired for CBF quantification, and for both ASL and rs-fMRI data a set of images with opposite phase encoding directions were collected for distortions correction. Subjects were asked to abstain from alcohol the day before and from caffeine the morning before each MRI exam. Subjects were instructed to lie still in the scanner, keep eyes closed but not fall asleep while the images were collected.

2.5. Functional connectivity preprocessing

The first 5 volumes were discarded to allow for magnetic field stabilization. Scans were corrected for distortions using the FMRIB's Software Library (FSL, fmrib.ox.ac.uk/fsl/) *topup* tool (Andersson and Sotiropoulos, 2016) and coregistered to the first scan. Additionally, data were scrubbed using ArtRepair toolbox (cibsr.stanford.edu/tools/human-brain-project/artrepair-software.html) for SPM12 (fil.ion.ucl.ac.uk/spm/software/spm12/). Scrubbing was performed on outlier volumes, defined as frames with excessive motion (>3 mm or >0.05°) or spikes in the global signal (>3% deviation from the mean) and per-slice corrected by temporal linear interpolation. Patients were excluded from further analysis when more than 25% of frames were classified as outliers after scrubbing. Subsequently, images were linearly spatially normalized to the Montreal Neurological Institute (MNI) template and spatially smoothed with a 6 mm FWHM. Non-neuronal sources of BOLD fluctuations were removed by regressing out the 6 rigid body head motion parameters and the signal from the CSF and white matter (WM) compartments, which were segmented from the T1-weighted scan and registered to the rs-fMRI space using SPM unified segmentation and affine registration. Finally, functional data were temporally high-pass filtered with a cut-off of 100 seconds (0.01 Hz) to reduce the effect of low-frequency drifts.

Changes in rs-fMRI connectivity were assessed through an independent component analysis (ICA) using the Group ICA Toolbox (GIFT version 3.0a). The number of independent components extracted (n = 30) was chosen according to the minimum description length criteria (Li et al., 2007). Networks were extracted from the pooled group of HC and patients (for patients both timepoints were considered). The resulting group maps were used to derive the corresponding individual components, through a back-reconstruction step. The estimated spatial maps were then converted into z-scores. The networks of interest (DMN and SN) were identified using a template matching spatial correlation procedure with standard templates (Shirer et al., 2012) through the FSL utility *fslcc*.

2.6. Arterial spin labeling preprocessing

ASL data were preprocessed and analyzed using FSL. Data were first realigned to account for spatial motion displacement and then corrected for nuisances (6 head motion parameters, CSF and WM signals) using linear regression. In addition, the ASL calibration scan was chosen as the reference image for estimating the coregistration parameters from ASL to the individual T1-weighted image by applying a rigid-body registration with 6° of freedom and Boundary-Based Registration cost function. Each T1-weighted image was also registered to the MNI space with 2-mm spatial resolution using a nonlinear method.

Preprocessed control and label volumes were pair-wise subtracted and averaged to obtain perfusion-weighted images, which were quantified into CBF [ml/100g/min] by applying the general kinetic model as follows:

$$CBF = \frac{6000 \cdot \lambda \cdot \Delta M \cdot e^{\frac{PLD}{T_{1b}}}}{2 \cdot \alpha \cdot \alpha_{inv} \cdot T_{1b} \cdot M_{0t} \cdot \left(1 - e^{\frac{-\tau}{T_{1b}}}\right)}$$

where λ is the brain-blood partition coefficient (0.9 mL/g), ΔM represents the perfusion-weighted maps, PLD is the postlabeling delay corrected for label decay in ascending slices acquired with 2D readout, T_{1b} is the longitudinal relaxation time of arterial blood (1650 ms at 3T), α is the labeling efficiency (0.85 for pCASL), α_{inv} corrects for the decrease in labeling efficiency due to 2 background suppression pulses (0.83) (Buxton et al., 1998). M_{0t} is the tissue equilibrium magnetization, voxel-wise estimated from the calibration scan, and τ represents the labeling duration (Alsop et al., 2015).

Considering the relatively low ASL spatial resolution and brain atrophy, partial volume corrected (PVC) CBF maps for grey matter were created for each subject. In detail, tissue probability maps derived from the segmentation of the individual T1-weighted image were first smoothed with a 3 × 3 × 4 mm^3 kernel to mimic the ASL resolution. These smoothed maps were then downsampled to the ASL space using the inverse of the previously estimated transformation matrix and finally applied to calculate the PVC CBF maps following the equation $CBF_{corr} = CBF_{uncorr}/(P_{gm} + 0.4 \cdot P_{wm})$ (Du et al., 2006). Finally, the joint ASL/T1-weighted and T1-weighted/MNI space transformation parameters were used to spatially normalize the estimated PVC CBF maps.

2.7. DTI processing

Data preprocessing was carried out with the FMRIB's Diffusion Toolbox (FDT, fsl.fmrib.ox.ac.uk/fsl/fslwiki/FDT), part of FSL. The *topup* tool was used to correct for susceptibility-induced distortions along with eddy to correct for eddy current-induced distortions and subject's motion. The DTIfit toolbox (part of FDT) was used to estimate the diffusion tensor and calculate fractional anisotropy (FA), mean (MD), axial (AxD), and radial (RD) diffusivity maps.

A tract-of-interest approach was used to measure the microstructural parameters (FA, MD, AxD, RD) within the WM tracts of the networks of interest. DMN and SN WM tract ROIs were defined using a previously published probabilistic atlas in MNI space (Figley et al., 2015). For each network, the WM probability maps (dorsal and ventral components of the DMN, anterior and posterior components of the SN) were thresholded at 25%, binarized, and combined to derive a single tract-mask for each network. Structural connectivity analysis was then carried out in the native diffusivity space of each subject, as follows. The Tract-Based Spatial Statistics (TBSS; fsl.fmrib.ox.ac.uk/fsl/fslwiki/TBSS) tool was used to compute the nonlinear transformations bringing native diffusion images into a standard reference space (Smith et al., 2006). The affine- and nonlinear transformations warping each subject's FA to a FA template in MNI space (FMRIB58_FA standard-space FA template) were computed using the FMRIB's Nonlinear Image Registration Tool (FNIRT, part of FSL). The inverse transformations were then computed and applied to each network ROI for back-projection from MNI space to each subject's diffusion space. The ROI analysis was restricted to the normal appearing WM by excluding WMHs and CSF voxels, as follows. WMHs were segmented from the FLAIR images using the lesion prediction algorithm (LPA) implemented in the LST toolbox (statistical-modelling.de/lst.html) (Schmidt et al., 2012). The T1 image of each subject was used as a reference image for co-registration before lesions' segmentation. Lesion probability maps were threshold at 0.95 and binarized. WMHs maps were then warped from T1 to DTI space by concatenating the nonlinear transformation bringing each subject's T1 image to the standard MNI template (computed with FSL FNIRT tool) with the inverse of the nonlinear warp bringing each DTI image to MNI space (computed with TBSS). The CSF was segmented from the MD maps using the FAST tool (part of FSL) and a 2-class segmentation.

2.8. Data analysis

The nonparametric Friedman test was used to evaluate the effect of time (T0 vs. T1) on clinical and cognitive variables, separately for each diagnostic group (AD and bvFTD) and tDCS protocol. For cognitive measures, a single composite score was computed for each domain by averaging the z-transformed scores according to the mean and SD of the HC group. Statistical significance was set at $p < 0.05$ using the Statistical Package for the Social Sciences (SPSS – Inc, version 23.0. Chicago).

For FC, the individual GIFT z-score maps of the DMN and the SN were thresholded at $z>2$ and the mean global FC was computed for each subject. For ASL, the thresholded FC maps were used as masks to compute the network mean CBF for each patient (Supplementary Figure S3). For DTI, average fractional anisotropy (FA), mean diffusivity (MD), axial diffusivity (AxD), and radial diffusivity (RD) were computed within the WM tracts connecting the nodes of each network of interest (i.e., the DMN and SN). To assess the effect of time, tDCS protocol, and network on FC, CBF, and DTI measures, linear models for repeated measures were performed including the 3 main effects and their interactions as predictors: (1) time, (2) protocol and (3) network as within-subject factors.

2.9. Monitoring of side effects

Adverse events were monitored through 2 structured questionnaires. A first questionnaire, administered at the end of the first and last tDCS sessions, was used to monitor the occurrence of the most common tDCS induced discomfort sensations and their intensity (Fertonani et al., 2015). A second questionnaire was administered to monitor adverse events occurring within 24 hours after each tDCS session.

3. Results

Twenty-six AD and 27 bvFTD patients were assessed for eligibility between June 2015 and July 2018 (Supplementary Figure S1). A sample of 20 HC was enrolled. Twenty-two AD and 23 bvFTD patients were randomized to either the anodal (11 AD; 12 bvFTD) or cathodal (11 AD; 11 bvFTD) tDCS protocol (Supplementary Table S1). Three patients were withdrawn by the investigators for safety reasons (i.e., psoriasis, $n = 1$; cortical vascular lesions on MRI, $n = 2$) and 2 patients withdrew from the study, leaving 10 patients in each group (Table 1; Supplementary Figure S1).

On average, patients performed MRI exam 4.5 ± 4.3 days before the first tDCS session, with no differences between AD (days 4.1 ± 3.9) and bvFTD (days 4.9 ± 4.7) ($p = 0.731$; $U = 268$). The MRI exam at follow-up was performed 3.4 ± 1.8 days after the last tDCS session with no differences between patient groups (AD: days 3.0 ± 0.2; bvFTD: 3.7 ± 2.5; $p = 0.758$; $U = 212$).

3.1. Cognitive and clinical measures

In AD, the aDMN protocol showed significant improvement in memory (+7%; delta mean T1-T0: 0.3 ± 0.2, $p = 0.002$) and language (+23%; delta mean T1-T0: 0.7 ± 0.6, $p = 0.01$; Table 2). Memory improvement was also reported in the cSN group (+6%; delta mean T1-T0: 0.3 ± 0.3, $p = 0.01$; Table 2). In bvFTD, we found a significant improvement in language in the aSN group (+16%; delta mean T1-T0: 0.7 ± 0.9, $p = 0.01$), whereas the cDMN group showed no cognitive changes (Table 2).

In AD, the aDMN protocol showed no significant effect in clinical variables (time effect: $p > 0.06$ for global CDR, CDR-SOB, NPI; Table 3). In the cSN protocol, no significant effect on CDR was reported (time effect: $p > 0.32$), whereas we found a significant improvement for NPI (30% improvement; delta mean T1-T0 of 3 ± 6, $p = 0.01$; Table 3). In bvFTD, the aSN protocol showed no effect on clinical measures (time effect: $p > 0.06$ for global CDR, CDR-SOB, NPI, FBI; Table 3). No improvement was reported for CDR in the cDMN group (time effect: $p = 1$), whereas NPI showed a significant improvement (20% improvement; delta mean T1-T0 of 6 ± 11, $p < 0.03$). No FBI effects were found ($p = 0.74$; Table 3).

3.2. Imaging network measures

3.2.1. Functional network connectivity

Rs-fMRI scans were available for 38 out of 40 patients ($n = 1$ bvFTD incomplete scan; $n = 1$ bvFTD excessive motion). In AD, no significant effect of time for either DMN or SN ($p > 0.90$) was found (Fig. 2, Supplementary Table S2). This null effect was due to a divergent pattern of FC changes between the 2 arms (Fig. 3). The linear model for repeated measure revealed a significant time*arm interaction for the DMN ($p = 0.009$), and a nonsignificant trend for the SN ($p = 0.17$), whereby the aDMN group showed FC changes in line with the hypothesis (i.e., DMN increases and SN decreases),

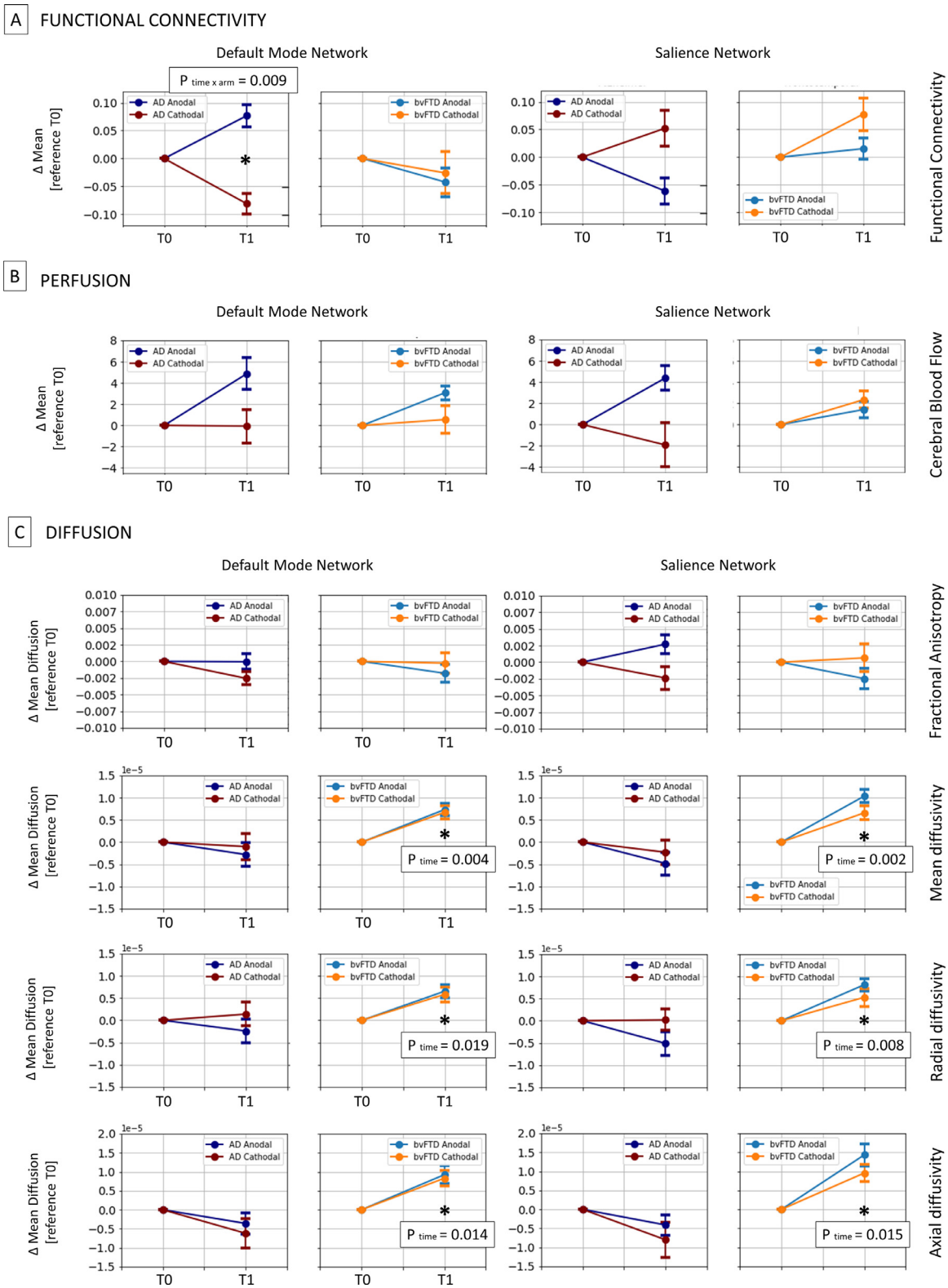

Fig. 2. Changes in imaging measures after tDCS in AD and bvFTD groups. Panel A) Functional connectivity: In AD a significant time*protocol interaction effect was found within the DMN, suggesting a divergent DMN modulation after the 2 tDCS paradigms. No significant effect was found in the bvFTD group; Panel B) Perfusion: No significant time or interaction effects were reported for both AD and bvFTD patients. Panel C) Diffusion: No significant time or interaction effects were reported for AD. No changes were reported in fractional anisotropy in bvFTD patients, whereas mean, radial and axial diffusivity in bvFTD showed a significant time effect. Significant results (marked with *) and standard error bars are reported. AD: aDMN protocol, dark blue; cSN protocol, dark red; bvFTD: aSN protocol, light blue; cDMN protocol, orange (For interpretation of the references to color in this figure legend, the reader is referred to the Web version of this article).

Table 1
Baseline sociodemographic and clinical characteristics of Alzheimer's disease (AD) and behavioral variant frontotemporal dementia (bvFTD) patients included in the study

	AD			bvFTD		
	aDMN n = 10	cSN n = 10	*p*	aSN n = 10	cDMN n = 10	*p*
Age	72 ± 6	73 ± 6	0.912	71 ± 10	69 ± 11	0.796
Sex (% Female)	60%	40%	0.371	30%	50%	0.361
Education	9 ± 3	8 ± 5	0.280	10 ± 4	8 ± 3	0.579
Onset age	68 ± 6	69 ± 6	0.912	66 ± 11	65 ± 10	0.739
MMSE	21 ± 2	21 ± 2	0.853	21 ± 5	23 ± 3	0.529
IADL (lost functions)	2 ± 2	2 ± 1	0.912	4 ± 3	4 ± 2	1
Barthel Index	99 ± 2	100 ± 0	0.481	94 ± 9	90 ± 12	0.436
GDS (30 items)	7 ± 3	6 ± 4	0.393	9 ± 9	9 ± 4	0.222
ARWMC scale	4.6 ± 1.6	5.8 ± 3.8	0.631	5.8 ± 4	4.6 ± 5.3[a]	0.274

Differences were assessed with the Wilcoxon signed-rank or chi-squared tests as appropriate.
Key: ARWMC, age-related white matter changes scale; GDS, geriatric depression scale; IADL, Instrumental activities daily living; MMSE, Mini mental state examination.
[a] Data available for 8 subjects.

Table 2
Changes in cognitive performance after brain network stimulation

	T0 Mean (SD)	Delta Mean (SD)	Time effect *p* value	T0 Mean (SD)	Delta Mean (SD)	Time effect *p* value
Alzheimer's disease (AD)						
	aDMN (n = 10)			cSN (n = 10)		
Memory	-4.4 (0.7)	0.3 (0.2)	*0.002*[a]	-4.7 (0.5)	0.3 (0.3)	*0.01*[a]
Language	-3.1 (1.6)	0.7 (0.6)	*0.01*[a]	-3.2 (1.3)	0.4 (0.6)	0.06
Executive Functions	-4.4 (3.5)	0.3 (2.9)	0.74	-5.6 (4.9)	-0.3 (2.4)	0.53
Visuospatial	-3.8 (2.5)	1.2 (1.1)	0.10	-3.2 (2.2)	0.0 (1.6)	0.53
Emotion Recognition	-1.6 (1.3)	0.1 (0.5)	1	-1.4 (1.4)	0.1 (0.6)	0.74
Behavioral variant frontotemporal dementia (bvFTD)						
	aSN (n = 10)			cDMN (n = 10)		
Memory	-4.0 (1.1)	0.1 (0.3)	0.21	-3.7 (1.1)	0.2 (0.3)	0.06
Language	-4.5 (2.2)	0.7 (0.9)	*0.01*[a]	-4.5 (1.6)	0.4 (0.6)	0.21
Executive Functions	-6.3 (6.3)	0.7 (2.3)	0.21	-5.5 (4.2)	-0.7 (1.6)	0.06
Visuospatial	-2.8 (1.8)	0.1 (0.8)	0.53	-3.7 (2.1)	0.4 (0.9)	0.21
Emotion Recognition	-3.2 (1.9)	0.3 (1.2)	0.21	-3.3 (1.3)	0.1 (0.9)	0.10

Nonparametric repeated measure ANOVA was used to assess time effect (Friedman test).
[a] Denotes statistically significant effects.

Table 3
Changes in clinical and behavioral scales after brain network stimulation

	T0 Mean (SD)	Delta Mean (SD)	Time effect *p* value	T0 Mean (SD)	Delta Mean (SD)	Time effect *p* value
Alzheimer's disease (AD)						
	aDMN (n = 10)			cSN (n = 10)		
CDR global score	0.7 (0.2)	-0.1 (0.2)	0.32	0.7 (0.3)	0.0 (0.0)	1
CDR-SOB score	3.2 (1.2)	0.1 (0.4)	1	3.3 (1.1)	0.0 (0.2)	0.32
NPI	11 (10)	-1 ± (3)	0.06	10 (7)	-3 (6)	*0.01*[a]
Behavioral variant frontotemporal dementia (bvFTD)						
	aSN (n = 10)			cDMN (n = 10)		
CDR global score	0.8 (0.3)	0.0 (0.0)	1	0.9 (0.6)	0.0 (0.0)	1
CDR-SOB score	4.6 (2.1)	-0.1 (0.3)	0.32	5.1 (3.3)	0.0 (0.0)	1
NPI	28 (15)	-1 (4)	0.06	30 (11)	-6 (11)	*0.03*[a]
FBI	26 (12)	-2 (4)	0.53	32 (6)	-4 (8)	0.74

Nonparametric repeated measure ANOVA was used to assess time effect (Friedman test).
Key: CDR, clinical dementia rating scale; CDR-SOB, clinical dementia rating scale – sum of boxes; NPI, neuropsychiatric inventory; FBI, frontal behavioral inventory.
[a] Denotes statistically significant effects.

whereas the cSN group showed the opposite pattern. The significance of the triple interaction time*arm*network ($p = 0.02$) confirmed the divergent pattern of DMN and SN networks across the 2 groups (Fig. 3, Supplementary Table S2). Within bvFTD patients, null time effects were reported for FC of the 2 networks (DMN and SN, $p > 0.16$; Fig. 2, Supplementary Table S2). Null time effects were not driven by protocol or network differences (protocol*time interaction and protocol*time*network interactions not significant; Supplementary Table S2).

3.2.2. Cerebral blood flow

ASL scans were available for 34 out of 40 subjects (6 data not available due to motion [n = 2] or incomplete data [n = 4]) including 18 AD (n = 9 for each arm) and 16 bvFTD (n = 7 for aSN and n = 9 for cDMN) for the analysis. We did not report a significant effect of time within the 2 networks, in either AD ($p > 0.30$) or bvFTD ($p > 0.10$; Fig. 2; Supplementary Table S2). In addition, no significant time*protocol*network interaction was found for AD ($p = 0.673$) and bvFTD ($p = 0.119$). Moreover, no sig-

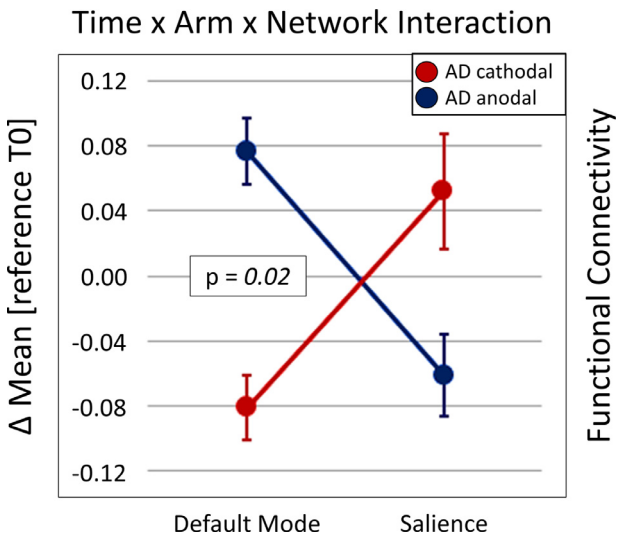

Fig. 3. Network interaction effect after tDCS in AD patients. In AD, a significant time*protocol*network effect was reported, showing a divergent effect of aDMN and cSN stimulation on functional connectivity.

nificant time*protocol interaction was reported in any diagnostic group (Supplementary Table S2).

3.2.3. Structural network connectivity

Diffusion MRI scans were available for 36 out of 40 patients (2 bvFTD were excluded due to incomplete scan, 2 bvFTD for artifacts/excessive motion). In AD, no significant effect was reported for all comparisons ($p > 0.2$; Fig. 2; Supplementary Table S3). In bvFTD no time effect was reported for FA ($p > 0.5$), whereas we observed a significant increase in MD (DMN: $p = 0.004$; SN: $p = 0.002$), combined with increases in both AxD and RD metrics ($p < 0.01$ for both networks; Fig. 2; Supplementary Table S3). By contrast, no time*protocol or time*protocol*network interactions were reported ($p > 0.4$), indicating that this effect was not driven by network or intervention (Supplementary Table S3).

3.3. Side effects

The incidence of adverse events was slightly higher in the cathodal arm than in the anodal arm (Supplementary Table S4), although the difference was not statistically significant ($\chi 2 = 2.23$; $p = 0.13$). All the reported adverse effects resolved within 24 hours. In general, tDCS was well tolerated by the patients. The most frequent discomfort sensation was pinching (n = 14), followed by itching (n = 5) and burning (n = 5). All of these discomfort perceptions were rated as mild (See supplementary Table S4). At T2, 1 bvFTD patient assigned to the cDMN arm dropped out of the study due to a serious adverse event occurring between T1 and T2 (intestinal infarction).

4. Discussion

This study assessing NIBS-induced clinical, cognitive, and network connectivity changes in AD and bvFTD using multimodal imaging suggests a divergent polarity-dependent effect of stimulation on clinical and cognitive measures. Specifically, our results suggest that cathodal tDCS stimulation of the SN in AD and of the DMN in bvFTD seems effective at improving behavior, whereas anodal tDCS stimulation of the disease-specific network (DMN in AD and SN in bvFTD) might restore cognition.

In AD, improvements in memory and language performance were observed after anodal DMN stimulation. The link between DMN and memory in AD is well established (Buckner et al., 2005) and our results suggest that this tDCS stimulation protocol may improve memory and other DMN-associated functions. Overall, the positive effect of anodal tDCS of the DMN on cognition coupled with the lack of clinical/behavioural effects suggests that this protocol might be more effective for cognitive rehabilitation than for clinical/behavioral recovery. Conversely, positive behavioral effects were reported in AD after cathodal tDCS stimulation of the SN. The SN plays a key role in modulating behavior (Seeley et al., 2007) and our findings in AD suggest that cathodal stimulation of this network might be effective in restoring SN-related symptoms. This finding is in line with previous evidence in major depression reporting an improvement of symptoms after prefrontal inhibition (Brunelin et al., 2014). Moreover, memory improvement was also observed in the cSN group, suggesting that suppression of the SN might have similar effects on memory.

A similar, sharp divergent clinical-cognitive pattern was observed in the bvFTD group: anodal tDCS stimulation of the SN resulted in no clear clinical benefit but cognitive improvement, whereas cathodal tDCS stimulation of the DMN improved behavioral symptoms but not cognition. These results are supported by reports of improvement in cognition but not in behavioral scores in bvFTD patients after anodal stimulation (Benussi et al., 2020). Overall, these divergent patterns suggest a trade-off between cognitive and behavioral effects after network stimulation through tDCS, as neither protocol outperformed the other.

This divergent clinical/cognitive pattern was echoed by rs-fMRI results in the AD cohort: anodal DMN stimulation was accompanied by positive DMN connectivity changes and concomitant decreases in SN, whereas cathodal SN stimulation showed opposite changes. The increase in DMN connectivity after anodal stimulation is in line with studies targeting key DMN hubs and reporting consistent changes in FC of the DMN (Antonenko et al., 2018; Keeser et al., 2011). Recently, in healthy adults, Antonenko et al. (2018) reported increased DMN after anodal stimulation targeting the right temporoparietal cortex associated with improved memory performance. Moreover, previous studies have reported that the effects of parietal stimulation might not be limited to the DMN, but may spread to other frontal networks, such as the SN (Hunter et al., 2015). These findings are in line with our results in the anodal DMN group. By contrast, although cathodal stimulation is often predicted to have inhibitory effects (Nitsche et al., 2003), cathodal-induced FC changes are less consistent compared to anodal stimulation. Polania et al. (2012) reported that cathodal tDCS over the motor cortex decreased FC in the cortico-striatal circuit. However, several studies reported opposite effects (i.e., increased FC) or no effect after cathodal stimulation (Amadi et al., 2014; Antonenko et al., 2017). Accordingly, our results suggest that a linear cathodal-inhibitory assumption may be too simplistic and that the effect of anodal versus cathodal stimulation on neuronal signal might involve other mechanisms, such as signal enhancement or noise reduction (Battaglini et al., 2017). Based on this model, we speculate that cathodal stimulation of the SN might cause a reduction of noise within the SN, thereby increasing its FC, and subsequently the interactions of the SN with the DMN. According to the triple network model (Menon, 2011), this may have caused a disengagement of the DMN, leading to a reduction of its FC. Conversely, anodal stimulation of the DMN might have strengthened its intrinsic correlation (signal enhancement mechanism), meanwhile decreasing connectivity of the SN. For both tDCS protocols, we speculate that symptoms improvement would be driven by an enhancement of FC of the corresponding network (DMN-cognition, SN-behavior). These interpretations,

however, should be taken with caution, since we detected no significant effect for the main factors, that is, time and protocol, but only a significant network*protocol*time interaction.

In bvFTD, the distinct clinical/cognitive patterns were not paralleled by divergent network FC changes (no significant interaction) and no effect of time and protocol was observed. This null effect might depend, at least partially, on structural connectivity alterations in the disease (Zhang et al., 2009). In the DTI analysis, we found a significant effect of time on MD, AxD and RD measures. Reshaping of FC after brain stimulation significantly depends on structural connectivity (Schintu et al., 2020) and although the coupling between structural and functional connectivity in dementia is poorly elucidated, it is possible that greater microstructural changes in bvFTD compared with AD (Zhang et al., 2009), might have reduced the effect of tDCS-induced network perturbation. Unexpectedly, we observed increased diffusivity in all directions after tDCS (i.e., increased MD, AxD, and RD). Changes in water diffusion may results from multiple biological processes, including changes in microstructure of connections (e.g., demyelination, axonal damage), increased extracellular volume, and/or increased membrane permeability (Beaulieu, 2002). These changes may reflect inflammatory response elicited by tDCS, which has been reported in animal models after anodal and cathodal tDCS (Rueger et al., 2012). Alternatively, increased diffusivity might indicate a faster spread of pathology along connections due to tDCS-induced axonal activation (Chakraborty et al., 2018). Clarifying these mechanisms is critical to understanding whether these tDCS effects are beneficial or detrimental.

Few studies have investigated the effect of tDCS on CBF to date. Studies in animals, controls, and MCI have reported an increase in CBF after anodal and/or a decrease in CBF after cathodal stimulation (Wachter et al., 2011; Stagg et al., 2013; Das et al., 2019), a trend similar to that observed in our AD population, albeit not significant. Similarly, in bvFTD aSN was associated with (not significantly) higher CBF values in the investigated networks. This pattern was also observed in the cDMN group. These results might suggest that in bvFTD, which generally exhibits marked hypoperfusion in frontal areas compared to AD (Hu et al., 2010), tDCS induces a weak increase in perfusion, regardless of the paradigm. However, these assumptions remain speculative, since CBF changes in AD and bvFTD were not significant. Further studies should assess the impact of tDCS network perturbation on CBF in these neurological diseases.

4.1. Limitations and strengths

The main limitation of our study is the small sample size, which limits the generalizability of the results. A second limitation is the lack of a placebo group. In this pilot study, we prioritized comparisons between anodal/cathodal groups and the analysis of the perturbation of the dynamic relationship between SN and DMN connectivity in AD and bvFTD. While the lack of a placebo group does not enable to assess “practice effect” caused by repeated testing of clinical and cognitive measures (Goldberg et al., 2015), this limitation would not impact imaging measures that are generally unaffected by practice effects. Moreover, while a traditional reference group was lacking, by implementing 2 active tDCS paradigms each protocol served as a reference for the other, similar to a previous study assessing DMN reorganization after brain stimulation (Eldaief et al., 2011). Notwithstanding these limitations, our study has 2 main strengths: (1) defining targets based on functional networks relevant to AD and bvFTD, and (2) collecting surrogate measures of network changes, thus providing direct measures of target engagement. Future NIBS studies could further improve this approach by developing personalized protocols to stimulate individual networks, for example, by computing the target from individual functional network maps.

5. Conclusion

Our study highlights the feasibility of designing noninvasive stimulation protocols targeting AD and bvFTD networks. Overall, patients showed changes on clinical and cognitive outcomes dependent on the stimulation protocol. While no difference was detected in functional network measures, in AD we observed a divergent FC pattern, suggesting that the 2 protocols elicit distinct clinical and biological responses. The choice of the best protocol for AD might thus depend upon the intended use (e.g., cognitive rehabilitation versus treatment of behavioral symptoms). While similar conclusions may apply to bvFTD, the observation of increased diffusivity after stimulation warrants further investigation to ascertain their impact on patients. These data further add to the body of evidence indicating the need to explore the complex nature between brain perturbation and functional organization to develop effective interventions in dementia.

Acknowledgements

This work was supported by the Italian Ministry of Health (Giovani Ricercatori grant GR2011–02349787, Ricerca Corrente). We thank Dr Siemon de Lange for his insightful discussion.

Data statement

The data supporting the conclusions of this study are publicly available at the following link: doi: 10.17632/j2gb8pcz2y.1.

Disclosure statement

The authors declare that they have no competing interests. The study was approved by the local ethics committee of the IRCCS Istituto Centro San Giovanni di Dio Fatebenefratelli in Brescia (Italy) (Number 43/2014; approval date September 8, 2014). Written informed consent was obtained from all participants. ClinicalTrials.gov identifier NCT03422250.

Author’s contributions

Conceptualization and funding acquisition: MP, FBP, and RM; methodology and analysis of data: LP, IBG, CF, MP, and GBF; acquisition of data and resources: LP, IBG, SG, AC, MSC, CG, OZ; tDCS procedure: EG, MC, and RM; writing—original draft: LP: supervision: MP; interpretation of data and review and editing of manuscript: FBP, IBG, CF, SG, MC, AC, MSC, CG, OZ, MC, MvDH, GBF, RM, and MP.

Supplementary materials

Supplementary material associated with this article can be found, in the online version, at doi:10.1016/j.neurobiolaging.2021.11.005.

References

Alsop, DC, Detre, JA, Golay, X, Hendrikse, J, Hernandez-Garcia, L, Lu, H, MacIntosh, BJ, Parkes, LM, Smits, M, van Osch, MJ, Wang, DJ, Wong, EC, Zaharchuk, G., 2015. Recommended implementation of arterial spin-labeled perfusion MRI for clinical applications: a consensus of the ISMRM perfusion study group and the European consortium for ASL in dementia. Magn. Reson. Med. 73, 102–116.

Amadi, U, Ilie, A, Johansen-Berg, H, Stagg, CJ., 2014. Polarity-specific effects of motor transcranial direct current stimulation on fMRI resting state networks. Neuroimage 88, 155–161.

Amodio, P, Wenin, H, Del Piccolo, F, Mapelli, D, Montagnese, S, Pellegrini, A, Musto, C, Gatta, A, Umiltà, C., 2002. Variability of trail making test, symbol digit test and line trait test in normal people. A normative study taking into account age-dependent decline and sociobiological variables. Aging Clin. Exp. Res. 14, 117–131.

Andersson, JLR, Sotiropoulos, SN., 2016. An integrated approach to correction for off-resonance effects and subject movement in diffusion MR imaging. Neuroimage 125, 1063–1078.

Antonenko, D, Külzow, N, Sousa, A, Prehn, K, Grittner, U, Flöel, A., 2018. Neuronal and behavioral effects of multi-day brain stimulation and memory training. Neurobiol. Aging 61, 245–254.

Antonenko, D, Schubert, F, Bohm, F, Ittermann, B, Aydin, S, Hayek, D, Grittner, U, Flöel, A., 2017. tDCS-Induced modulation of GABA levels and resting-state functional connectivity in older adults. J. Neurosci. 37, 4065–4073.

Battaglini, L, Noventa, S, Casco, C., 2017. Anodal and cathodal electrical stimulation over V5 improves motion perception by signal enhancement and noise reduction. Brain. Stimul. 10, 773–779.

Beaulieu, C., 2002. The basis of anisotropic water diffusion in the nervous system - a technical review. NMR Biomed 15, 435–455.

Benedictus, MR, Leeuwis, AE, Binnewijzend, MA, Kuijer, JP, Scheltens, P, Barkhof, F, van der Flier, WM, Prins, ND., 2017. Lower cerebral blood flow is associated with faster cognitive decline in Alzheimer's disease. Eur. Radiol 27, 1169–1175.

Benussi, A, Dell'Era, V, Cosseddu, M, Cantoni, V, Cotelli, MS, Cotelli, M, Manenti, R, Benussi, L, Brattini, C, Alberici, A, Borroni, B., 2020. Transcranial stimulation in frontotemporal dementia: a randomized, double-blind, sham-controlled trial. Alzheimers Dement. (N Y) 6, 12033.

Bikson, M, Name, A, Rahman, A., 2013. Origins of specificity during tDCS: anatomical, activity-selective, and input-bias mechanisms. Front. Hum. Neurosci. 7, 688.

Biswal, B, Yetkin, FZ, Haughton, VM, Hyde, JS., 1995. Functional connectivity in the motor cortex of resting human brain using echo-planar MRI. Magn. Reson. Med. 34, 537–541.

Brunelin, J, Jalenques, I, Trojak, B, Attal, J, Szekely, D, Gay, A, Januel, D, Haffen, E, Schott-Pethelaz, AM, Brault, C, Poulet, E.STEP Group, 2014. The efficacy and safety of low frequency repetitive transcranial magnetic stimulation for treatment-resistant depression: the results from a large multicenter French RCT. Brain Stimul. 7, 855–863.

Buckner, RL, Snyder, AZ, Shannon, BJ, LaRossa, G, Sachs, R, Fotenos, AF, Sheline, YI, Klunk, WE, Mathis, CA, Morris, JC, Mintun, MA., 2005. Molecular, structural, and functional characterization of Alzheimer's disease: evidence for a relationship between default activity, amyloid, and memory. J. Neurosci 25, 7709–7717.

Buxton, RB, Frank, LR, Wong, EC, Siewert, B, Warach, S, Edelman, RR., 1998. A general kinetic model for quantitative perfusion imaging with arterial spin labeling. Magn. Reson. Med. 40, 383–396.

Caffarra, P, Vezzadini, G, Dieci, F, Zonato, F, Venneri, A., 2002. Rey-Osterrieth complex figure: normative values in an Italian population sample. Neurol. Sci. 22, 443–447.

Caffarra, P, Gardini, S, Zonato, F, Concari, L, Dieci, F, Copelli, S, Freedman, M, Stracciari, A, Venneri, A., 2011. Italian norms for the Freedman version of the clock drawing test. J. Clin. Exp. Neuropsychol 33, 982–988.

Carlesimo, GA, Caltagirone, C, Gainotti, G., 1996. The mental deterioration battery: Normative data, diagnostic reliability and qualitative analyses of cognitive impairment. The group for the standardization of the Mental Deterioration Battery. Eur. Neurol. 36, 378–384.

Chakraborty, D, Truong, DQ, Bikson, M, Kaphzan, H, 2018. Neuromodulation of axon terminals. Cereb. Cortex. 28, 2786–2794.

Cummings, JL, Mega, M, Gray, K, Rosenberg-Thompson, S, Carusi, DA, Gornbein, J., 1994. The neuropsychiatric inventory: comprehensive assessment of psychopathology in dementia. Neurology 44, 2308–2314.

Das, N, Spence, JS, Aslan, S, Vanneste, S, Mudar, R, Rackley, A, Quiceno, M, Chapman, SB., 2019. Cognitive training and transcranial direct current stimulation in mild cognitive impairment: a randomized pilot trial. Front. Neurosci 13, 307.

Day, GS, Farb, NA, Tang-Wai, DF, Masellis, M, Black, SE, Freedman, M, Pollock, BG, Chow, TW., 2013. Salience network resting-state activity prediction of frontotemporal dementia progression. JAMA Neurol. 70, 1249–1253.

DeTure, MA, Dickson, DW., 2019. The neuropathological diagnosis of Alzheimer's disease. M*ol. Neurodegener* 14, 32.

Dodich, A, Cerami, C, Canessa, N, Crespi, C, Marcone, A, Arpone, M, Realmuto, S, Cappa, SF., 2014. Emotion recognition from facial expressions: a normative study of the Ekman 60-faces test in the Italian population. Neurol. Sci. 35, 1015–1021.

Du, AT, Jahng, GH, Hayasaka, S, Kramer, JH, Rosen, HJ, Gorno-Tempini, ML, Rankin, KP, Miller, BL, Weiner, MW, Schuff, N., 2006. Hypoperfusion in frontotemporal dementia and Alzheimer disease by arterial spin labeling MRI. Neurology 67, 1215–1220.

Eldaief, MC, Halko, MA, Buckner, RL, Pascual-Leone, A., 2011. Transcranial magnetic stimulation modulates the brain's intrinsic activity in a frequency-dependent manner. Proc. Natl. Acad. Sci. U S A. 108, 21229–21234.

Ferri, CP, Prince, M, Brayne, C, Brodaty, H, Fratiglioni, L, Ganguli, M, Hall, K, Hasegawa, K, Hendrie, H, Huang, Y, Jorm, A, Mathers, C, Menezes, PR, Rimmer, E, Scazufca, M, 2005. Alzheimer's Disease International. Global prevalence of dementia: a Delphi consensus study. Lancet 366, 2112–2117.

Fertonani, A, Ferrari, C, Miniussi, C., 2015. What do you feel if I apply transcranial electric stimulation? Safety, sensations and secondary induced effects. Clin. Neurophysiol. 126, 2181–2188.

Figley, TD, Bhullar, N, Courtney, SM, Figley, CR., 2015. Probabilistic atlases of default mode, executive control and salience network white matter tracts: an fMRI-guided diffusion tensor imaging and tractography study. Front. Hum. Neurosci 9, 585.

Folstein, MF, Folstein, SE, McHugh, PR., 1975. "Mini-mental state". A practical method for grading the cognitive state of patients for the clinician. J. Psychiatr. Res. 12, 189–198.

Fox, MD, Buckner, RL, Liu, H, Chakravarty, MM, Lozano, AM, Pascual-Leone, A., 2014. Resting-state networks link invasive and noninvasive brain stimulation across diverse psychiatric and neurological diseases. Proc. Natl. Acad. Sci. U S A 111, E4367–E4375.

Giovagnoli, AR, Del Pesce, M, Mascheroni, S, Simoncelli, M, Laiacona, M, Capitani, E., 1996. Trail making test: normative values from 287 normal adult controls. Ital. J. Neurol. Sci. 17, 305–309.

Goldberg, TE, Harvey, PD, Wesnes, KA, Snyder, PJ, Schneider, LS., 2015. Practice effects due to serial cognitive assessment: Implications for preclinical Alzheimer's disease randomized controlled trials. Alzheimers Dement. (Amst) 1, 103–111.

Hu, WT, Wang, Z, Lee, VM, Trojanowski, JQ, Detre, JA, Grossman, M., 2010. Distinct cerebral perfusion patterns in FTLD and AD. Neurology 75, 881–888.

Hunter, MA, Coffman, BA, Gasparovic, C, Calhoun, VD, Trumbo, MC, Clark, VP., 2015. Baseline effects of transcranial direct current stimulation on glutamatergic neurotransmission and large-scale network connectivity. Brain Res. 1594, 92–107.

Hughes, CP, Berg, L, Danziger, WL, Coben, LA, Martin, RL., 1982. A new clinical scale for the staging of dementia. Br. J. Psychiatry 140, 566–572.

Keeser, D., Meindl, T., Bor, J., Palm, U., Pogarell, O., Mulert, C., Brunelin, J., Moller, H.J., Reiser, M., Padberg, F., 2011. Prefrontal transcranial direct current stimulation changes connectivity of resting-state networks during fMRI. J. Neurosci. 31, 15293 15284e.

Kertesz, A, Davidson, W, Fox, H., 1997. Frontal behavioral inventory: diagnostic criteria for frontal lobe dementia. Can. J. Neurol. Sci. 24, 29–36.

Koch, G, Bonnì, S, Pellicciari, MC, Casula, EP, Mancini, M, Esposito, R, Ponzo, V, Picazio, S, Di Lorenzo, F, Serra, L, Motta, C, Maiella, M, Marra, C, Cercignani, M, Martorana, A, Caltagirone, C, Bozzali, M., 2018. Transcranial magnetic stimulation of the precuneus enhances memory and neural activity in prodromal Alzheimer's disease. Neuroimage 169, 302–311.

Laird, AR, Fox, PM, Eickhoff, SB, Turner, JA, Ray, KL, McKay, DR, Glahn, DC, Beckmann, CF, Smith, SM, Fox, PT., 2011. Behavioral interpretations of intrinsic connectivity networks. J. Cogn. Neurosci. 23, 4022–4237.

Lawton, MP, Brody, EM., 1969. Assessment of older people: self-maintaining and instrumental activities of daily living. Gerontologist 9, 179–186.

Lefaucheur, JP, Aleman, A, Baeken, C, Benninger, DH, Brunelin, J, Di Lazzaro, V, Filipović, SR, Grefkes, C, Hasan, A, Hummel, FC, Jääskeläinen, SK, Langguth, B, Leocani, L, Londero, A, Nardone, R, Nguyen, JP, Nyffeler, T, Oliveira-Maia, AJ, Oliviero, A, Padberg, F, Palm, U, Paulus, W, Poulet, E, Quartarone, A, Rachid, F, Rektorová, I, Rossi, S, Sahlsten, H, Schecklmann, M, Szekely, D, Ziemann, U., 2020. Evidence-based guidelines on the therapeutic use of repetitive transcranial magnetic stimulation (rTMS): an update (2014-2018). Clin. Neurophysiol. 131, 474–528.

Lefaucheur, JP, Antal, A, Ayache, SS, Benninger, DH, Brunelin, J, Cogiamanian, F, Cotelli, M, De Ridder, D, Ferrucci, R, Langguth, B, Marangolo, P, Mylius, V, Nitsche, MA, Padberg, F, Palm, U, Poulet, E, Priori, A, Rossi, S, Schecklmann, M, Vanneste, S, Ziemann, U, Garcia-Larrea, L, Paulus, W., 2017. Evidence-based guidelines on the therapeutic use of transcranial direct current stimulation (tDCS). Clin. Neurophysiol. 128, 56–92.

Li, YO, Adali, T, Calhoun, VD., 2007. Estimating the number of independent components for functional magnetic resonance imaging data. Hum. Brain. Mapp. 28, 1251–1266.

Lin, J, Lin, LA, Sandkoh, S., 2016. A general overview of adaptive randomization design for clinical trials. J. Biom. Biostat. 07, 2.

Lindenberg, R, Sieg, MM, Meinzer, M, Nachtigall, L, Floel, A., 2016. Neural correlates of unihemispheric and bihemispheric motor cortex stimulation in healthy young adults. Neuroimage 140, 141–149.

Lorenzi, M, Beltramello, A, Mercuri, NB, Canu, E, Zoccatelli, G, Pizzini, FB, Alessandrini, F, Cotelli, M, Rosini, S, Costardi, D, Caltagirone, C, Frisoni, GB., 2011. Effect of memantine on resting state default mode network activity in Alzheimer's disease. Drugs. Aging 28, 205–217.

Mackenzie, IR, Neumann, M., 2016. Molecular neuropathology of frontotemporal dementia: insights into disease mechanisms from postmortem studies. J. Neurochem 138, 54–70.

Mahoney, FI, Barthel, DW., 1965. Functional evaluation: the barthel index. Md. State Med. J. 14, 61–65 12.

McKhann, GM, Knopman, DS, Chertkow, H, Hyman, BT, Jack, CR, Kawas, CH, Klunk, WE, Koroshetz, WJ, Manly, JJ, Mayeus, R, Mohs, RC, Morris, JC, Rossor, MN, Scheltens, P, Carrillo, MC, Thies, B, Weintraub, S, Phelps, C, 2011. The diagnosis of dementia due to Alzheimer's disease: recommendations from the National Institute on Aging-Alzheimer's Association workgroups on diagnostic guidelines for Alzheimer's disease. Alzheimers Dement. 7, 263–269.

Meinzer, M, Lindenberg, R, Phan, MT, Ulm, L, Volk, C, Flöel, A., 2015. Transcranial direct current stimulation in mild cognitive impairment: behavioral effects and neural mechanisms. Alzheimers Dement. 11, 1032–1040.

Menon, V., 2011. Large-scale brain networks and psychopathology: a unifying triple network model. Trends Cogn. Sci. 15, 483–506.

Menon, V, Uddin, LQ., 2010. Saliency, switching, attention and control: a network model of insula function. Brain Struct. Funct. 214, 655–667.

Monaco, M, Costa, A, Caltagirone, C, Carlesimo, CA., 2013. Forward and backward span for verbal and visuo-spatial data: standardization and normative data from an Italian adult population. Neurol. Sci. 43, 749–754.

Neary, D, Snowden, J, Mann, D., 2005. Frontotemporal dementia. Lancet Neurol. 4, 771–780.
Nitsche, MA, Liebetanz, D, Antal, A, Lang, N, Tergau, F, Paulus, W., 2003. Modulation of cortical excitability by weak direct current stimulation–technical, safety and functional aspects. Suppl. Clin. Neurophysiol 56, 255–276.
Novelli, G, Papagno, C, Capitani, E, Laiacona, M, Cappa, SF, Vallar, G., 1986a. Tre test clinici di memoria verbale a lungo termine. Taratura su soggetti normali. Arch. Psicol. Neurol. Psichiatr. 47, 278–296.
Novelli, G, Papagno, C, Capitani, E, Laiacona, M, Cappa, SF, Vallar, G., 1986b. Tre test clinici di produzione lessicale. Taratura su soggetti normali. Arch. Psicol. Neurol. Psichiatr. 47, 477–506.
Ozdemir, RA, Tadayon, E, Boucher, P, Momi, D, Karakhanyan, KA, Fox, MD, Halko, MA, Pascual-Leone, A, Shafi, MM, Santarnecchi, E., 2020. Individualized perturbation of the human connectome reveals reproducible biomarkers of network dynamics relevant to cognition. Proc. Natl. Acad. Sci. U S A. 117, 8115–8125.
Palop, JJ, Mucke, L., 2016. Network abnormalities and interneuron dysfunction in Alzheimer disease. Nat. Rev. Neurosci. 17, 777–792.
Pezzulo, G, Zorzi, M, Corbetta, M., 2021. The secret life of predictive brains: what's spontaneous activity for? Trends Cogn. Sci. 25, 730–743.
Pievani, M, Pini, L, Cappa, SF, Frisoni, GB., 2016. Brain networks stimulation in dementia: insights from functional imaging. Curr. Opin. Neurol. 29, 756–762.
Pievani, M, Pini, L, Ferrari, C, Pizzini, FB, Boscolo Galazzo, I, Cobelli, C, Cotelli, M, Manenti, R, Frisoni, GB, 2017. Coordinate-based meta-analysis of the default mode and salience network for target identification in non-invasive brain stimulation of Alzheimer's disease and behavioral variant frontotemporal dementia networks. J. Alzheimers Dis. 57, 825–843.
Pini, L, Pizzini, FB, Cotelli, M, Manenti, R, Frisoni, GB, Pievani, M., 2018. Non-invasive brain stimulation in dementia: a complex network story. Neurodegener. Dis. 18, 281–301.
Pini, L, Youssov, K, Sambataro, F, Bachoud-Levi, AC, Vallesi, A, Jacquemot, C., 2020. Striatal connectivity in pre-manifest Huntington's disease is differentially affected by disease burden. Eur. J. Neurol. 27, 2147–2157.
Pini, L, Wennberg, AM, Salvalaggio, A, Vallesi, A, Pievani, M, Corbetta, M., 2021. Breakdown of specific functional brain networks in clinical variants of Alzheimer's disease. Ageing Res. Rev. 72, 101482 *In Press*.
Polanía, R, Paulus, W, Nitsche, MA., 2012. Modulating cortico-striatal and thalamo-cortical functional connectivity with transcranial direct current stimulation. Hum. Brain Mapp. 33, 2499–2508.
Poreisz, C, Boros, K, Antal, A, Paulus, W., 2007. Safety aspects of transcranial direct current stimulation concerning healthy subjects and patients. Brain Res. Bull. 72, 208–214.
Ranganath, C, Ritchey, M., 2012. Two cortical systems for memory-guided behaviour. Nat. Rev. Neurosci. 13, 713–726.
Rascovsky, K, Hodges, JR, Knopman, D, Mendez, MF, Kramer, JH, Neuhaus, J, van Swieten, JC, Seelaar, H, Dopper, EG, Onyike, CU, Hillis, AE, Josephs, KA, Boeve, BF, Kertesz, A, Seeley, WW, Rankin, KP, Johnson, JK, Gorno-Tempini, ML, Rosen, H, Prioleau-Latham, CE, Lee, A, Kipps, CM, Lillo, P, Piguet, O, Rohrer, JD, Rossor, MN, Warren, JD, Fox, NC, Galasko, D, Salmon, DP, Black, SE, Mesulam, M, Weintraub, S, Dickerson, BC, Diehl-Schmid, J, Pasquier, F, Deramecourt, V, Lebert, F, Pijnenburg, Y, Chow, TW, Manes, F, Grafman, J, Cappa, SF, Freedman, M, Grossman, M, Miller, BL., 2011. Sensitivity of revised diagnostic criteria for the behavioural variant of frontotemporal dementia. Brain 134, 2456–2477.
Rueger, MA, Keuters, MH, Walberer, M, Braun, R, Klein, R, Sparing, R, Fink, GR, Graf, R, Schroeter, M., 2012. Multi-session transcranial direct current stimulation (tDCS) elicits inflammatory and regenerative processes in the rat brain. PLoS One 7, e43776.
Sale, MV, Mattingley, JB, Zalesky, A, Cocchi, L., 2015. Imaging human brain networks to improve the clinical efficacy of non-invasive brain stimulation. Neurosci. Biobehav. Rev. 57, 187–198.
Sandrini, M, Umiltà, C, Rusconi, E., 2011. The use of transcranial magnetic stimulation in cognitive neuroscience: a new synthesis of methodological issues. Neurosci. Biobehav. Rev. 35, 516–536.
Schintu, S, Cunningham, CA, Freedberg, M, Taylor, P, Gotts, SJ, Shomstein, S, Wassermann, EM., 2020. Callosal anisotropy predicts attentional network changes after parietal inhibitory stimulation. Neuroimage 226, 117559.
Shine, JM, Bissett, PG, Bell, PT, Koyejo, O, Balsters, JH, Gorgolewski, KJ, Moodie, CA, Poldrack, RA., 2016. The dynamics of functional brain networks: integrated network states during cognitive task performance. Neuron 92, 544–554.
Schmidt, P, Gaser, C, Arsic, M, Buck, D, Förschler, A, Berthele, A, Hoshi, M, Ilg, R, Schmid, VJ, Zimmer, C, Hemmer, B, Mühlau, M., 2012. An automated tool for detection of FLAIR-hyperintense white-matter lesions in Multiple Sclerosis. Neuroimage 59, 3774–3783.
Seeley, WW, Crawford, RK, Zhou, J, Miller, BL, Greicius, MD., 2009. Neurodegenerative diseases target large-scale human brain networks. Neuron. 62, 42–52.
Seeley, WW, Menon, V, Schatzberg, AF, Keller, J, Glover, GH, Kenna, H, Reiss, AL, Greicius, MD., 2007. Dissociable intrinsic connectivity networks for salience processing and executive control. J. Neurosci 27, 2349–2356.
Serafin, M, Surian, L., 2004. Il Test degli Occhi: uno strumento per valutare la "teoria della mente. G. Ital. Psicol. 4, 839–862.
Shirer, WR, Ryali, S, Rykhlevskaia, E, Menon, V, Greicius, MD., 2012. Decoding subject-driven cognitive states with whole-brain connectivity patterns. Cereb. Cortex. 22, 158–165.
Smith, SM, Jenkinson, M, Johansen-Berg, H, Rueckert, D, Nichols, TE, Mackay, CE, Watkins, KE, Ciccarelli, O, Cader, MZ, Matthews, PM, Behrens, TE., 2006. Tract-based spatial statistics: voxelwise analysis of multi-subject diffusion data. Neuroimage 31, 1487–1505.
Stagg, CJ, Bachtiar, V, Amadi, U, Gudberg, CA, Ilie, AS, Sampaio-Baptista, C, O'Shea, J, Woolrich, M, Smith, SM, Filippini, N, Near, J, Johansen-Berg, H, 2014. Local GABA concentration is related to network-level resting functional connectivity. Elife 3, e01465.
Spinnler, H, Tognoni, G., 1987. Standardizzazione e Taratura italiana di test neuropsicologici. Ital. J. Neurol. Sci. 6 (1), 120 Suppl 8 to.
Sridharan, D, Levitin, DJ, Menon, V., 2008. A critical role for the right fronto-insular cortex in switching between central-executive and default-mode networks. Proc. Natl. Acad. Sci. U. S. A 105, 12569–12574.
Stagg, CJ, Lin, RL, Mezue, M, Segerdahl, A, Kong, Y, Xie, J, Tracey, I., 2013. Widespread modulation of cerebral perfusion induced during and after transcranial direct current stimulation applied to the left dorsolateral prefrontal cortex. J. Neurosci 33, 11425–11431.
Wachter, D, Wrede, A, Schulz-Schaeffer, W, Taghizadeh-Waghefi, A, Nitsche, MA, Kutschenko, A, Rohde, V, Liebetanz, D., 2011. Transcranial direct current stimulation induces polarity-specific changes of cortical blood perfusion in the rat. Exp. Neurol. 227, 322–327.
Wang, JX, Rogers, LM, Gross, EZ, Ryals, AJ, Dokucu, ME, Brandstatt, KL, Hermiller, MS, Voss, JL., 2014. Targeted enhancement of cortical-hippocampal brain networks and associative memory. Science 345, 1054–1057.
Yesavage, JA, Brink, TL, Rose, TL, Lum, O, Huang, V, Adey, M, VO, Leirer, 1982. Development and validation of a geriatric depression screening scale: a preliminary report. J. Psychiatr. Res. 17, 37–49.
Zhang, HY, Wang, SJ, Liu, B, Ma, ZL, Yang, M, Zhang, ZJ, Teng, GJ., 2010. Resting brain connectivity: changes during the progress of Alzheimer disease. Radiology 256, 598–606.
Zhang, Y, Schuff, N, Du, AT, Rosen, HJ, Kramer, JH, Gorno-Tempini, ML, Miller, BL, Weiner, MW., 2009. White matter damage in frontotemporal dementia and Alzheimer's disease measured by diffusion MRI. Brain 132, 2579–2592.
Zhou, J, Greicius, MD, Gennatas, ED, Growdon, M, Jang, JY, Rabinovici, GD, Kramer, JH, Weiner, M, Miller, BL, Seeley, WW., 2010. Divergent network connectivity changes in behavioural variant frontotemporal dementia and Alzheimer's disease. Brain 133, 1352–1367.